Theor Chem Acc (2003) 109:170–175
DOI 10.1007/s00214-002-0405-3

Theoretical Chemistry Accounts

Regular article

Computational insight into the effect of C(19) substituents on [1,7]-hydrogen shift in previtamin D

Olga Dmitrenko[1], **Robert D. Bach**[1], **Rafal R. Sicinski**[2], **Wolfgang Reischl**[3]

[1] Department of Chemistry and Biochemistry, University of Delaware, Delaware, USA
[2] Department of Chemistry, University of Warsaw, Warsaw, Poland
[3] Department of Chemistry, University of Vienna, Vienna, Austria

Received: 17 May 2002 / Accepted: 11 September 2002 / Published online: 14 February 2003

Abstract. B3LYP calculations in conjunction with natural bond orbital population analysis have been performed for a previtamin D model and corresponding transition structures for the [1,7]-hydrogen migration. In addition the 19,19-difluoro, 19-methoxy and 19-fluoro substituted analogs were investigated. The calculated activation barriers decrease in the following order: $CHF_2 > CH_3 > CH_2OCH_3$ (24.8, 23.5 and 20.1 kcal/mol). This is in qualitative agreement with experiments. It has been suggested that a decrease of the barrier by a 19-methoxy substituent and its increase by a 19,19-difluoro substituent are phenomena of different origin. In the case of 19-methoxy substitution, the effect is due to the charge redistribution in the triene system and the decrease of the C(19)–H bond energy. The effect of two fluorine substituents at C-19 on the activation barrier is suggested to originate from the combination and balance of several factors: electrostatic repulsion between the negative fluorine atom and the π-electron cloud over the conjugated system, an increase of the HOMO–LUMO gap, and geminal difluoro substitution affecting C–F and C–C bond energies.

Keywords: Vitamin D – Density functional calculations – Orbital–orbital interactions – Bond dissociation energies – G2 calculations

Introduction

One of the key reactions of the in vivo and in vitro synthesis of vitamin D is the thermal interconversion previtamin D↔vitamin D (Scheme 1) via the [1,7]-antarafacial hydrogen shift [1]. This reaction is widely reviewed in most textbooks of organic chemistry or natural products chemistry. Nevertheless, the mechanistic aspects on the effects of substituents, in particular at C-19, are still unclear. The effects of methoxy, acetoxy and fluorine substituents at C-19 on the [1,7]-hydrogen migration in previtamin D analogs have been studied experimentally in the last 20 years by several groups in the USA and in Europe. In all these studies, it has been found that a 19,19-difluoro substituent completely inhibits the reaction, whereas 19-methoxy and 19-acetoxy substituents accelerate the conversion of previtamin D to vitamin D [1, 2, 3, 4, 5].[1]

In spite of the experimental agreement, the mechanistic interpretations of these opposite effects were controversial [1, 2, 3, 4, 5]. Sialom and Mazur [3] discussed electron-donating/withdrawing and inductive effects; possible steric effects were also suggested. The complete inhibition of thermal isomerization for 19, 19-difluoro substitution was explained by a strong inductive effect of the two fluorine atoms [3] on the basis of analogy to known [1,5]-hydrogen shift reactions [6] and the assumption that a localized positive charge on the terminal carbon atom of the triene system is involved in the transition structure for the [1,7]-hydrogen migration. However, in other studies [5], it has been concluded that inductive effects do not play an important role in the stability of 19-acetoxy and 19-methoxy vitamin D analogs. It was also questioned whether the thermal stability of 19,19-difluoroprevitamin D could be attributed to the

Contribution to the 8th Electronic Computational Chemistry Conference, 2002

Electronic Supplementary Material to this paper (full text of the lecture in html as given at the ECCC8 conference) can be obtained by using the SpringerLink server located at http://dx.doi.org/10.1007/s00214-002-0405-3.

Correspondence to: O. Dmitrenko
e-mail: odmitr@udel.edu

[1] An exceptionally high thermal instability was observed for the C(19)-methoxy and C(19)-acetoxy substituted previtamins D. In C(19)-difluoro previtamin D, no thermal isomerization to the respective vitamin D derivative could be detected [3]. The rate constants for thermal [1,7]-hydrogen shift are not available.

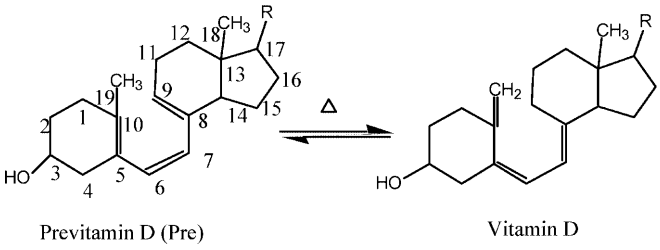

Scheme 1

strong inductive effect [5] of the fluorine atoms. More recently, effects of electron-donating methoxy substituents and electron-withdrawing fluoride substituents on the [1,5]-hydrogen shift were studied in several model 1,3-pentadienes [7]. It was suggested that decreasing the electron density of the π-system destabilizes the aromatic transition state (TS) and increases the activation energy. Importantly, it was suggested that not only inductive effects, but also orbital–orbital and steric interactions may affect the energetics of this pericyclic reaction [7].

In order to get insight into possible electronic effects of the C-19 substituent in the reactions of the [1,7]-hydrogen shift in C(19)-modified previtamin D analogs, we performed gas-phase density functional calculations using the B3LYP hybrid method [9, 10, 11]. As discussed in the literature, this method produces satisfactory results for predicting the activation energies for the [1,5]-hydrogen shift in 1,3-pentadiene and for the antarafacial [1,7]-hydrogen shift in simple previtamin D model systems [8].

The present study is focused on gas-phase reactivity, structural and electronic features of the relatively large previtamin D model 1 and its C(19)-fluoro and C(19)-methoxy modified analogs **2**–**4** (Scheme 2). The model was chosen as to include the entire steroid skeleton with is crucial *trans*-hydridane system. The reasons for omitting the 3-hydroxyl group in our present calculations are discussed in detail in Ref. [12].

The growing awareness of the importance of interactions between filled and unfilled orbitals [13] has

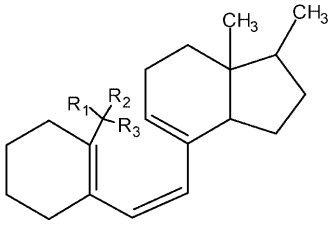

1 $R_1 = R_2 = R_3 = H$

2 $R_1 = R_3 = F$, $R_2 = H$

3 $R_1 = OCH_3$, $R_2 = R_3 = H$

4 a $R_1 = F$, $R_2 = R_3 = H$ *(exo)*
4 b $R_1 = R_2 = H$, $R_3 = F$ *(endo)*

Scheme 2

encouraged us also to examine the possible correlation between relative energies of natural bond orbitals (NBO), orbital interactions [14] and the activation barriers for the C(19)-substituted systems.

Computational methods

Density functional studies and ab initio molecular orbital calculations [15] were performed with Gaussian 98 system of programs [16]. For the NBO analysis, the NBO 4.0 module of Gaussian 98 was used. The Becke three-parameter hybrid functional [9] combined with the Lee, Yang and Parr correlation functional [10], denoted B3LYP [11], was employed in the calculations using density functional theory. The geometries were optimized [17] at the B3LYP level using the 6-31G(d) basis set. For the nonsubstituted system, all stationary points were characterized by frequency calculations. Homolytic bond energies and the energies of dehydrogenation reactions ($\Delta \boldsymbol{E}$, kilocalories per mole) quoted in the text are derived from G2 total energies, while bond dissociation energies (BDE) are derived from $\Delta \boldsymbol{H}(298)$ [18].[2]

Results and discussion

The three lowest-energy transition structures (TS-**1**, TS-**2**, TS-**3**, see Fig. 1) and the corresponding previtamin D model minima [12, 19] (GS-**1**, GS-**2**, GS-**3**) have been fully optimized.[3]

The reaction in the parent model system **1** ($R_1 = R_2 = H$) is characterized by a classical barrier of 23.5 kcal/mol. This is 1.3 kcal/mol lower than in compound **2** ($R_1 = R_2 = F$) and 3.4 kcal/mol higher than in methoxy-substituted **3**. The comparison of the distances between migrating hydrogen (H_t) and carbon atoms 9 and 19 in the transition structures suggests that TS-**3** is an early TS, whereas TS-**2** is a late TS. This is in agreement with the calculated barriers for these reactions. Nevertheless, the [1,7]-hydrogen migration in system **2** is not consistent with the Hammond postulate[4]. The calculated reaction barriers are qualitatively in line with the experimental observations [1, 2, 3] that the methoxy substituent significantly accelerates the reac-

[2] The G2 method is generally considered to be reliable to about 1.2 kcal/mol for the molecule set of 125 compounds used to calibrate the method.

[3] Each system has four transition structures that differ in the A-ring conformation (3β-hydrogen can be axial or equatorial) and helicity of the triene system (right-handed, *P* chirality and left-handed, *M* chirality). To reduce the overall effort and save computational time, we carried out optimization of models that have the 3β-hydrogen only in the equatorial position. We believe that such a restriction of the A-ring conformational flexibility does not affect significantly the triene portion of the system and the relative energetics of the transition structures for the [1,7]-hyrogen shift. We found that in the gas-phase, TSs with a *P*-helix are always lower in energy by 2.2 kcal/mol in **1** and **2** and 3.6 kcal/mol in **3** at the B3LYP/6-31G(d) level of theory. Previtamin D has at least eight low-energy (within 2 kcal/mol) ground-state conformations that differ in their configuration around single bonds C(5)–C(6) and C(7)–C(8), the sign of their corresponding dihedral angles, and in their A-ring conformations (axial versus equatorial orientation of 3β–OH).

[4] On the basis of the 3-desoxy (3β-H-equatorial) vitamin D model we estimated the overall (from global reactant minimum to global product minimum) reaction exothermicity of $\Delta E = 4$ kcal/mol at the B3LYP/6-31G(d) level of theory. See Ref. [12] for more conformational details of previtamin D and vitamin D molecules. In order to check the consistency with the Hammond postulate, we also calculated reaction energies for models **1**–**3** based upon total B3LYP/6-31G(d) energies directly involved in [1,7]-hydrogen migration prereaction and postreaction folded conformers (local minima on the reaction pathway connected to TS). It was found that the reaction energies for systems **1**, **2** and **3** are 5.9, 2.9 and −1.8 kcal/mol. This supports (based upon the Hammond postulate) the lowering of the barrier by the 19-methoxy substituent (system **3**), but rather provides opposite expectations (to the experiment) for system **2**.

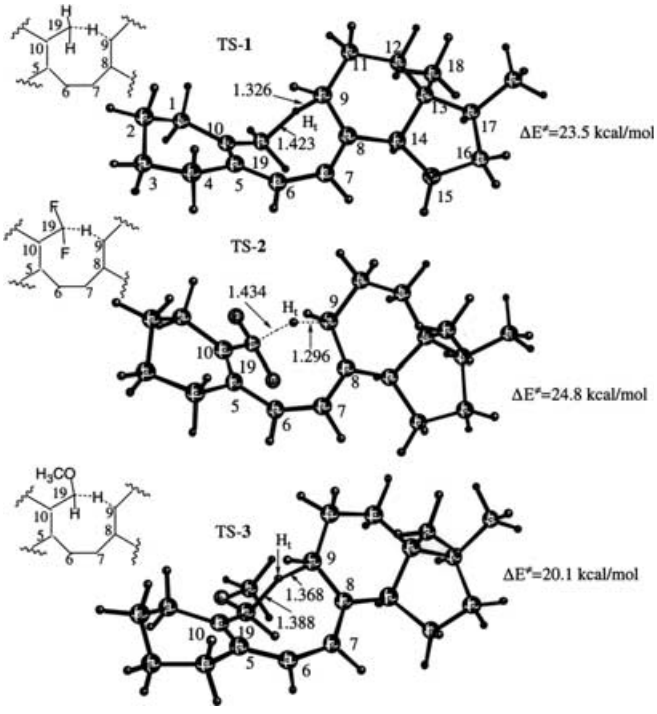

Fig. 1. Transition structures for the [1,7]-hydrogen shift in 3-desoxy previtamin D model **1** and its analogs with 19-difluoro (**2**) and 19-methoxy (**3**) substituents optimized at the B3LYP 6-31G(d) level of theory. The activation barriers are calculated with respect to the corresponding global ground-state minima of the (−)tZ(+)c geometry of the triene system (seco-B-ring). The distances shown are in angstroms

tion, whereas difluoro substitution completely inhibits the hydrogen migration [3]. Nevertheless, we are aware that experiments are performed in solvents and other solvent-induced effects could be of some importance for this type of reaction. Thus, it should be emphasized that the present study is aimed at analyzing intramolecular electronic effects of C(19) substituents without possible external medium-dependent factors.

The first and most logical assumption about the origin of the opposite effects of methoxy and fluoro substituents at C-19 could be their different electron-donating/withdrawing properties that may change the electron distribution in the triene system in opposite directions. Surprisingly, the calculated charges do not support these expectations. Both cases show dramatic effects on the charge distribution, in particular, on the C-19 atom (Table 1). But these data indicate the same trend of changes (both substituents withdraw electrons from C-19). Moreover, in the 19-difluoro model **2**, the net NBO charge on C-19 is positive for the ground-state minimum (0.6*e*) and the TS (0.7*e*), whereas in model **3**, these charges are still negative (as in model **1**), but significantly decreased (−0.1*e* in GS-**3** and −0.01*e* in TS-**3**). In the ground-state minima GS-**2** and GS-**3** and transition structures TS-**2** and TS-**3**, the charges on carbon atoms 5, 7 and 9 were increased relative to the parent model **1** (GS-**1**, TS-**1**), whereas on carbons 6, 8 and 10 they were decreased. On the basis of the charges (Table 1), one may even expect that owing to electrostatic repulsion between the leaving hydrogen (H_t) and the positively charged C-19 (0.6 in GS-**2**) the cleavage of the C(19)–H bond should be significantly easier in comparison with the two other models **1** and **3**.

In the NBO study of ground-state (+c)Z(+)c conformers GS-**1**, GS-**2** and GS-**3**, our interests were focused on the C(8)–C(9) π bond, the C(19)–H_t σ bond and the corresponding antibonding orbitals (antibonds) since they should be affected in the primary stage of the [1,7]-hydrogen shift. Also we analyzed the lowest-energy occupied and highest-energy unoccupied NBOs. We found that in all three TSs there are two comparable stabilizing interactions between filled and unfilled orbitals of C(8)–C(9) and C(19)–H_t bonds, π–σ^* and σ–π^* interactions. In both cases, i.e., difluoro- and methoxy-substitution at C-19, these energetic contributions are slightly larger than in parent system **1**.

The NBO energies for the C(8)–C(9) π, C(5)–C(10) π and C(19)–H_t σ bonds and the corresponding antibonding orbitals are summarized in Table 2.

While the energy gap between the lowest-energy occupied and the highest-energy unoccupied NBOs in GS-**1** and GS-**3** is about the same (195.2 and 194.8 kcal/mol), it is 9.4 kcal/mol larger for GS-**2** owing to the lowering of the C(5)–C(10) π-bond energy by the difluoro substituent at C19. A similar comparison of the HOMO–LUMO energy gaps using population analysis based upon the self-consistent-field density indicates the same trend: the largest HOMO–LUMO energy gap is found for GS-**2** (113.3 kcal/mol), whereas the values for GS-**1** and GS-**3** are comparable (111.8 and 111.1 kcal/mol). Thus, these observations provide some explanation for the increase of the barrier in model system **2**: the larger the HOMO–LUMO energy gap, the less reactive the molecule is. Interestingly, the difluoro substitution at C-19 causes a remarkable increase of the energy gap between the filled C(19)–H_t σ orbital and the unfilled C(8)–C(9) π orbital ($\Delta\Delta E\sigma\pi^* = 37.0$ kcal/mol) in contrast to the case of substitution with the 19-methoxy group ($\Delta\Delta E\sigma\pi^* = 4.3$ kcal/mol). This is mainly due to stabilization of the filled C(19)–H_t σ orbital in GS-**2**, which indicates reduced reactivity of this bond.

This prompted us to analyze the possible effect of both substituents on the C(19)–H bond dissociation energy at the G2 level of theory [20] using small model molecules (ethane, its difluoro and methoxy derivatives).[5] The bond energy data given in Table 3 suggest that the proximity of oxygen reduces the homolytic BDE of C–H by about 6 kcal/mol, whereas the two fluorine substituents do not affect the C–H bond dissociation energy. This provides an explanation for the reduced barrier for the [1,7]-hydrogen shift in 19-methoxy substituted previtamin D (**3**) since the weaker C(19)–H bond can be broken more easily (providing earlier TS) owing to the presence of the neighboring oxygen. The comparison of the proton affinities (PA) of the migrating hydrogen atom (H_t) in the analogs investigated is also informative. The previtamin D model **1** in its

[5] Calculated G2 bond energies are typically 2 kcal/mol higher than experimental BDEs.

Table 1. Natural bond orbital (*NBO*) charges (B3LYP/6-31G*) on carbon atoms of the triene system and migrating hydrogen in the previtamin D model **1** and its 19-substituted analogs (**2** and **3**) in the ground state (*GS*) and the corresponding transition structures (*TS*). All the GS (GS minimum) charge data are calculated for the (+)cZ(+)c conformers

	TS-**1** 10β–CH_3	TS-**2** –CHF_2	TS-**3** –CH_2OCH_3	GS-**1** 10β–CH_3	GS-**2** –CHF_2	GS-**3** –CH_2OCH_3
C(19)	−0.570	0.688	−0.011	−0.690	0.607	−0.112
C(10)	−0.024	−0.150	−0.058	0.009	−0.104	−0.014
C(5)	−0.068	−0.049	−0.061	−0.075	−0.028	−0.063
C(6)	−0.223	−0.238	−0.246	−0.213	−0.223	−0.216
C(7)	−0.261	−0.233	−0.254	−0.224	−0.201	−0.223
C(8)	−0.006	−0.006	−0.035	−0.064	−0.062	−0.067
C(9)	−0.397	−0.391	−0.376	−0.187	−0.199	−0.186
H_t	0.269	0.234	0.244	0.237	0.187	0.201

Table 2. Calculated NBOs and energies (au) for selected bonds in GS-**1**, GS-**2** and GS-**3** (+)cZ(+)c-conformers [B3LYP/6-31G(d)]. An *asterisk* indicates an antibonding orbital. The energy difference between interacting bonding and antibonding NBOs is given in kilocalories per mole, $\Delta E\pi\sigma^* = E_{\sigma^*[C(19)-H]} - E_{\pi[C(8)-C(9)]}$; $\Delta E\sigma\pi^* = E_{\pi^*[C(8)-C(9)]} - E_{\sigma[C(19)-H]}$. $\Delta E\pi\pi^*$ is highest occupied NBO (*HONBO*)–lowest unoccupied NBO (*LUNBO*) gap (kcal/mol). HONBO and LUNBO energies (au) are given in *bold*

	GS-1 10β–CH_3	GS-2 –CHF_2	GS-3 –CH_2OCH_3
π [C(8)–C(9)]	−0.248	**−0.256**	−0.251
π [C(5)–C(10)]	**−0.241**	−0.259	**−0.244**
π^* [C(8)–C(9)]	0.082	0.075	0.077
π^* [C(5)–C(10)]	**0.070**	**0.070**	**0.067**
σ [C(19)–H]	−0.478	−0.540	−0.489
σ^* [C(19)–H]	0.454	0.439	0.435
$\Delta E\pi\sigma^*$	440.2	436.0	430.6
$\Delta E\sigma\pi^*$	351.2	386.2	355.5
$\Delta E\pi\pi^*$	195.2	204.6	194.8

Table 3. Calculated homolytic CH, CC and CF bond energies and bond dissociation energies (*BDE*, kcal/mol) at the G2 level of theory for the ethane and ethylene molecule and its difluoro- and methoxy-substituted analogs

	Bond type	ΔE (G2)	BDE (G2) ΔH^0_{298}
CH_3CH_2–H	C–H	100.9	102.6
CH_3CF_2–H	C–H	100.9	102.5
CH_3CH_2–F	C–F	114.2	115.7
CH_3CFH–F	C–F	123.0	124.3
CH_3(CH–H)OCH_3	C–H	95.0	96.6
CH_2CH–H	C–H	110.5	112.0
CH_2CH–F	C–F	125.2	126.5
CH_2CF–F	C–F	130.2	131.5
CH_3–CH_3	C–C	88.3	90.8
CH_3–CFH_2	C–C	92.2	94.3
CH_3–CF_2H	C–C	96.8	98.7
CFH_2–CFH_2	C–C	93.3	94.9

(+)cZ(+)c conformation has an estimated PA_{Ht} of 389.5 kcal/mol [B3LYP/6-31G(d); zero-point-energy correction has not been included]. At the same theoretical level, 19-methoxy model **3** has a reduced PA_{Ht} of 383.5 kcal/mol, consistent with easier homolytic C(19)–H bond cleavage. This is supported by the NBO charge distribution as well. The reduction in the electron density around C-19 in GS-**3** and TS-**3** in comparison with the parent system **1** is calculated (Table 1). Thus, the more electronegative methoxy substituent tends to destabilize the reacting polarized C(19)–H^{δ} [7].

On the basis of the charge distribution, as well as bond orbital and bond dissociation energy analyses, one may rather expect a decrease of the reaction barrier in both these cases or at least no effect in the case of the 19-difluoro substituted analog. Inspection of the structure of TS-**2** indicates that one of the fluorine atoms is in close proximity to the triene system (the distances between the fluorine atom and the olefinic carbon atoms are smaller than 2.9 Å). This may suggest that the repulsion between the fluorine atom and the negatively charged π cloud over the triene system destabilizes the transition structure, thereby raising the reaction barrier.[6] In order to test this assumption the monosubstituted 19-fluoro model **4** was studied. We optimized the global minimum GS-**4** with the (−)tZ(+)c conformation which is similar to those found for GS-**1**, GS-**2** and GS-**3**. Two transition structures TS-**4a** and TS-**4b** were located and characterized by the exo and endo orientation of the fluorine atom with respect to the triene system (Fig. 2).

As expected the two TSs differ in their reaction barrier. For TS-**4a** the reaction barrier is lowered to 21.6 kcal/mol, but rotating the fluorine atom into the endo orientation causes a destabilization of TS-**4b** by 2.0 kcal/mol ($\Delta E^{\ddagger} = 23.5$ kcal/mol). Thus, without electrostatic repulsion (TS-**4a**), the 19-fluoro substitution decreases the reaction barrier with respect to parent model **1**, whereas C–F/π-cloud interaction destabilizes the transition state TS-**4b** up to the level of TS-**1**.

The presence of a second fluorine atom in model **2** provides an additional destabilization effect (by about 1–2 kcal/mol) as evidenced by the higher barrier of 24.8 kcal/mol (Fig. 1). The idea of the geminal difluoro substitution can potentially be gleaned from the energies of dehydrogenation reactions of model alkanes (Eqs. 1, 2, 3, 4) calculated at the G2 level of theory:

The comparison of the Eqs. 1 and 2 provides an indication that two geminal fluorine atoms give rise to a marked higher reaction endothermicity (by about 4 kcal/mol). The other two equations (Eqs. 3, 4) suggest that dehydrogenation of monofluoro- and, in particular, methoxy- substituted ethanes is an energetically less demanding process. There are at least two significant

[6] Owing to strong electrostatic repulsions in **2**, the GS-**2** anion structure of the (+)cZ(+)c geometry was destabilized and no local minimum in that region was located.

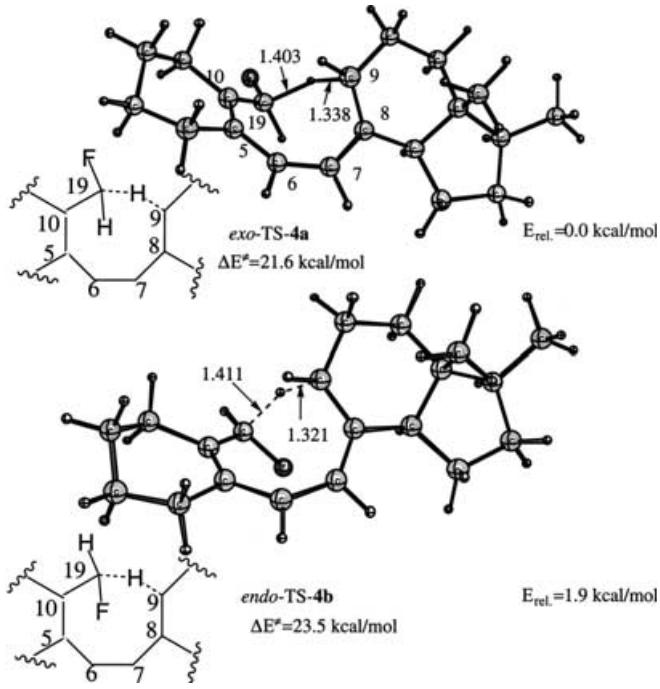

Fig. 2. Transition structures for the [1,7]-hydrogen shift in 3-desoxy previtamin D model **4** with 19-fluoro substituent in *exo*-TS-**4a** and *endo*-TS-**4b** positions with respect to the triene system [B3LYP/6-31G(d)]. *endo*-TS-**4b** is 1.9 kcal/mol higher in energy than *exo*-TS-**4a**. The activation barriers are calculated with respect to the corresponding common global ground-state minimum of the (−)tZ(+)c geometry of the triene system (seco-B-ring). The distances shown are in angstroms

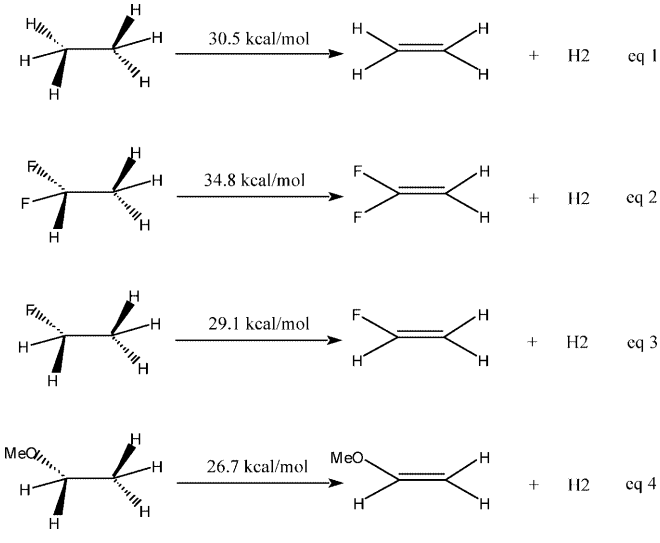

factors affecting the energetics of dehydrogenation reactions in monofluoro and difluoro substituted ethanes (Eqs. 2, 3), C–F and C–C/C = C bond energies (Table 3). These contributions act in opposite directions; thus, their balance determines the outcome. In general, these equations demonstrate that the presence of the second fluorine atom in the geminal position could make a significant contribution to the inhibiting effect of difluoro substitution in the previtamin D system.

Conclusions

The gas-phase B3LYP/6-31G(d) calculations performed in this study suggest that 19-methoxy and 19,19-difluoro substituent effects observed in previtamin D thermal isomerization to corresponding vitamin D have different origins.

The comparisons of the G2 bond dissociation energies for smaller model molecules, as well as NBO charge distributions in the systems **1**–**3** and their corresponding transition structures for the [1,7]-hydrogen shift provide an understanding for the significant acceleration of the reaction in the 19-methoxy previtamin D model (based upon the weakening of the C(19)–H bond by electron withdrawal).

The effect of 19,19-difluoro substitution has a more complex origin and combines electrostatic and orbital contributions.

The calculated effect of the transition structure destabilization in 19-fluoro-substituted previtamin D model **4b** with a fluorine-atom at the endo position versus model **4a** with a fluorine atom distant from the triene system has an electrostatic origin. It is suggested that this effect is partially responsible for the increase of the reaction barrier in 19,19-difluoro substituted model **2**. The increase of the HOMO–LUMO energy gap in GS-**1** is considered to be another factor responsible for the decrease of 19, 19-difluoro substituted previtamin D reactivity.

Model dehydrogenation reactions and the corresponding G2 energetics provide additional insight. It is suggested that the presence of the second fluorine atom at C-19 (in the geminal position) may play a significant role in the inhibition effect of [1,7]-hydrogen migration.

Acknowledgements. This work was supported by the Osterreichische Nationalbank (Jubiläumsfondsprojekt Nr. 7395 to W.R.) and by the National Science Foundation (CHE-01380 to R.D.B). We are also thankful to the University of Vienna Computer Center and the National Center for Supercomputing Applications Urbana, Illinois and Lexington, Kentucky, for generous amounts of computer time.

References

1. Havinga E (1973) Experientia 29: 1181
2. (a) Akhtar M, Gibbons CJ (1965) J Chem Soc 1101; (b) Moriarty RM, Paaren HE (1980) Tetrahedron Lett 2389; (c) Moriarty RM, Paaren HE (1981) J Am Chem Soc 46: 970
3. Sialom B, Mazur Y (1980) J Org Chem 45: 2201
4. Rodewald WJ, Sicinski RR (1983) Pol J Chem 57: 1267
5. Sicinski RR (1992) Acta Chim Hung 129: 191
6. Breslow R, Hoffman JH, Perchonock C (1973) Tetrahedron Lett 3723
7. Saettel NJ, Wiest O (2000) J Org Chem 65: 2331
8. (a) Hess BA (2001) J Org Chem 66: 5897; (b) Hess BA, Schaad LJ, Pancir J (1985) J Am Chem Soc 107:149; (c) Okamura WH, Elnagar HY, Ruther M, Dobreff S (1993) J Org Chem 58: 600
9. (a) Becke AD (1988) Phys Rev A 38: 3098; (b) Becke AD (1993) J Chem Phys 98: 5648
10. Lee C, Yang W, Parr RG (1988) Phys Rev B37: 785
11. Stevens PJ, Devlin FJ, Chablowski CF, Frisch MJ (1994) J Phys Chem 80: 11623
12. Dmitrenko O, Frederick JH, Reischl W (2000) J Mol Struct (THEOCHEM) 530: 85
13. Michl J, West R (2000) Acc Chem Res 33: 821

14. Wienhold F (1998) In: Schleyer PvR (ed) The encyclopedia of computational chemistry. Wiley, Chichester, p 1792
15. Hehre WJ, Radom L, Schleyer PvR, Pople JA (1986) Ab initio molecular orbital theory. Wiley, New York
16. Frisch MJ, Trucks GW, Schlegel HB, Scuseria GE, Robb MA, Cheeseman JR, Zakrzewski VG, Montgomery JA, Stratmann RE, Burant JC, Dapprich S, Millam JM, Daniels AD, Kudin KN, Strain MC, Farkas O, Tomasi J, Barone V, Cossi M, Cammi R, Mennucci B, Pomelli C, Adamo C, Clifford S, Ochterski J, Petersson GA, Ayala PY, Cui Q, Morokuma K, Malick DK, Rabuck AD, Raghavachari K, Foresman JB, Cioslowski J, Ortiz JV, Baboul AG, Stefanov BB, Liu G, Liashenko A, Piskorz P, Komaromi I, Gomperts R, Martin RL, Fox DJ, Keith T, Al-Laham MA, Peng CY, Nanayakkara A, Gonzalez C, Challacombe M, Gill PMW, Johnson B, Chen W, Wong MW, Andres JL, Gonzalez C, Head-Gordon M, Replogle ES, Pople JA (1998) Gaussian 98, revision A.7. Gaussian, Pittsburgh, PA
17. (a) Schlegel HB (1982) J Comput Chem 3: 214; (b) Schlegel HB (1987) Adv Chem Phys 67: 249; (c) Schlegel HB (1994) In: Yarkony DR (ed) Modern electronic structure theory. World Scientific. Singapore, p 459
18. (a) Curtiss LA, Raghavachari K, Trucks GW, Pople JA (1991) J Chem Phys 94: 7221; (b) Curtiss LA, Raghavachari K, Pople JA (1997) J Chem Phys 106: 1063
19. (a) Dauben WG, Funhoff DJH (1988) J Org Chem 53: 5070; (b) Dmitrenko O, Reischl W (1996) Monatsh Chem 127: 445; (c) Dmitrenko OG, Terenetskaya IP, Reischl W (1997) J Photochem Photobiol A 104: 113; (d) Dmitrenko O, Reischl W (1998) J Mol Struct (THEOCHEM) 431: 229; (e) Dmitrenko O, Reischl W, Vivian JT, Frederick JH (1999) J Mol Struct (THEOCHEM) 467: 195; (f) Dmitrenko O, Frederick JH, Reischl W (2001) J Photochem Photobiol A 139: 125
20. (a) Bach RD, Dmitrenko O (2002) J Org Chem 67(8): 2588; (b) Bach RD, Dmitrenko O (2002) J Org Chem 67: 3884